Mineralogical Magazine, October 2017, Vol. 81(5), pp. 1223–1244

A re-examination of water in agate and its bearing on the agate genesis enigma

Terry Moxon

55 Common Lane, Auckley, Doncaster DN9 3HX, UK

[*Received 15 June 2016; Accepted 30 November 2016; Associate Editor: Martin Lee*]

ABSTRACT

Dehydration of silanol and molecular water in 60 agates from 12 hosts with ages between 23 to 2717 Ma has been investigated using desiccators and high-temperature furnace heating. There are wide differences in the water data obtained under uncontrolled and fixed atmospheric water vapour pressure conditions. After agate acclimatization at 20°C and 46% relative humidity, the total water (silanol and molecular) was determined in powders and mini-cuboids by heating samples at 1200°C. Agates from hosts < 180 Ma all showed a greater mass loss using powders and demonstrate that after prolonged high-temperature heating, silanol water is partially-retained by the mini-cuboids. Desiccator dehydration of powders and slabs shows that powder preparation can produce water losses; this is particularly relevant in agates from hosts < 180 Ma. The identified problems have consequences for water quantification in agate and chalcedony using infrared or thermogravimetric techniques. Mobile and total water in agate is considered in relation to host-rock age, mogánite content and crystallite size. Links are observed between the various identified water contents allowing comment on quartz development and agate genesis. The water data also supports previous claims that agates from New Zealand and Brazil were formed long after their host.

Keywords: agate, chalcedony, silanol, water, relative humidity, genesis, mogánite.

Introduction

Agate and chalcedony are microcrystalline members of the quartz family of minerals which can be divided into two groups based upon their petrographic textural features. In cross-polarized light, thin sections of jasper, flint and chert typically reveal a mainly granular microstructure, whereas chalcedony shows a fibrous form. Agate is banded or variegated chalcedony. Although fibrosity is the characteristic petrographic observation of agate and chalcedony, it has never been observed with the scanning electron microscope (SEM). Instead, a fractured agate surface displays a globular morphology. The commonly observed white banding contrasts against this globular background by appearing as a stacked plate edge-like structure, which is more developed in agates from hosts with ages > 50 Ma (Moxon, 2002).

Agate has a high degree of silica purity, generally > 97 wt.%, with non-volatile impurities < 1 wt.% (Götze, *et al.*, 2001). Whereas, chalcedony and agate are predominately α-quartz they also include mogánite: another silica polymorph that is ubiquitous in all agates which have not been subject to metamorphic activity or laboratory heating. Detection of mogánite in microcrystalline quartz usually requires identification by powder X-ray diffraction (XRD). Mogánite recognition can be difficult at low concentrations as a wide distribution results in a limited contribution to the Bragg reflection (Götze, *et al.*, 1998). Indeed, agate from hosts > 300 Ma can appear to be mogánite free using XRD. Raman spectroscopy readily identifies trace mogánite, which has been detected in agate from hosts as old as 1100 Ma (Moxon *et al.*, 2007).

Questions about agate genesis have been asked for more than 200 years. There have been few

E-mail: moxon.t@tiscali.co.uk
https://doi.org/10.1180/minmag.2017.081.002

definitive answers, apart from a consensus on the agate formation temperature in basic igneous hosts of <100°C (Fallick *et al.*, 1985, Saunders, 1990). Chert and silica sinter have generated a much greater literature leading to a well-recognized diagenetic sequence starting with amorphous silica and finishing with α-quartz. Development details have been summarized for chert (Knauth, 1994) and silica sinter (Rogers *et al.*, 2004) and utilized for agate in the Landmesser (1995, 1998) model as the following sequence:

$$\text{Amorphous silica} \rightarrow \text{cristobalite/tridymite} \rightarrow \text{cristobalite} \rightarrow (\pm\text{chalcedony} + \text{mogánite}) \rightarrow \text{granular quartz} \quad (1)$$

Water is the major impurity in agate, existing as both free (H_2O) and silanol water (Si–OH) giving a total water concentration as high as ~1.8 wt.% (Flörke *et al.*, 1982). The nature of water in agate is however, complex. Water can exist as individual molecules although hydrogen bonding creates trapped water clusters. Silanol water exists individually but is also linked by hydrogen bonding with either neighbouring silanol groups or water molecules. Sites for free water include intergranular regions, structural defects and trapped fluid inclusions, whereas silanol groups are to be found mainly on surfaces and as structural defects (e.g. Yamagishi *et al.*, 1997; Fukuda *et al.*, 2009). The water content in the microcrystalline quartz family has been determined in a large number of studies. More recent studies include agate (Moxon *et al.*, 2013); chalcedony (Schmidt *et. al.*, 2013); flint (Schmidt, 2014); jasper (Hemantha Kumar *et al.*, 2010). Thermogravimetric analysis (TGA) and/or infrared techniques are the usual methods of water quantification.

The present investigation was initiated after small slabs and powders from the same Brazilian agate slice were stored in a desiccator but gave different percentage mass losses. The first objective of the study was to establish the extent of water loss differences between agate slabs and powders. Secondly, part way through the study, it was apparent that water mobility in agate slabs varied with the relative humidity. By default, data from these uncontrolled surroundings could be compared with fresh slabs from the same agates after acclimatization under controlled conditions. The third objective was to examine any relationship between the determined water data and agate host-rock age. Finally, water plays an essential role in transporting silica into the gas vesicle and in quartz crystallite development during agate ageing. This dual water role is considered in relation to the genesis enigma. Apart from relative humidity measurements, all percentages are wt.% and data in parentheses are ± one standard deviation.

Samples and methods

Origin of agate samples

Apart from the Las Choyas agates, the samples investigated are the common wall-lining type found in basic igneous hosts with an age range from 23 to 2717 Ma (Table 1). Some of the agates selected have been characterized previously providing knowledge of their crystallite size, mogánite, and apparent water content (Moxon and Carpenter, 2009 and references therein). The 12 agate regions are considered as four groups on the basis of the age of the host-rock. The host-rocks listed in Table 1 are considered in groups described as 'young' (23 to 135 Ma), 'middle age' (180 to 275 Ma), 'old' (412 to 1100 Ma) and Archaean (2717 Ma).

Young agate hosts are from Mt. Warning, Queensland, Australia (23 Ma); Ojo Laguna, Mexico (38 Ma); Las Choyas, Mexico (45 Ma); Isle of Rum, Scotland (60 Ma); Mt. Somers, New Zealand (89 Ma); Rio Grande do Sul, Brazil (135 Ma). Mt. Warning agates are white- to- pale brown with weak banding that are in contrast to the wide variety of vivid colours shown by the Mexican Laguna agates. Las Choyas agates are exported worldwide with the hollow type described as coconut geodes. The solid near-spherical agates used in the study are limited to blends of white, blue-grey and grey. These agates, up to 12 cm diameter, occur in the vitric tuff of the Liebres Formation. Rum agates are white/cream with poor banding and are smaller but similar in appearance to the Mt. Somers, New Zealand agates. The Brazilian samples could be from a very wide area as they consist of purchased batches from the Soledado mines and a UK mineral dealer. Brazilian agates are readily surface dyed but none of the study samples had been artificially dyed. Natural samples are characterized by shades of brown to near grey with sizes commonly >15 cm.

Middle-age agate hosts are from Bobonong, Botswana (180 Ma); Bay of Fundy, Nova Scotia, Canada (202 Ma) and Agate Creek, Queensland, Australia (275 Ma). Botswana is just one of a handful of countries that produce sufficient agate for world export. The agates are found in gravel accumulations and riverbeds and are collected for

https://doi.org/10.1180/minmag.2017.081.002 Published online by Cambridge University Press

TABLE 1. Agate samples used for the determination of water content.

Region and collector*	Age of host† (Ma)	Site or Formation, rock host, sample number
Mt. Warning, Queensland, Australia (JR)	23	Oxley River, basalt, 1,2,6,7,8
Chihuahua, Mexico (BC)	38	Rancho El Agate, andesite, 1,12,13,15,17
Las Choyas, Mexico (JC,BC)	45	Liebres Formation, vitric tuff, 6,9,11,15,17
Mt. Somers, New Zealand (VT)	89	Woolshed Creek, basalt, 12,13,14,17,18
Rum, Scotland (RL)	60	Northern Rum, basalt, 1,2,3,12,13
Rio Grande do Sul Brazil & UK purchase	135	Soledado mines, basalt, 12,39,64,72,75
Bobonong, Semolale, Botswana (HK)	180	Karoo volcanics, basalt, 33,80,112,114,152
Nova Scotia, Canada (BI)	202	Bay of Fundy, basalt, 11,21,24,25,30
Queensland, Australia (NC,DA)	275	Agate Creek, basalt, 104,108,122,140,142
Eastern Midland Valley, Scotland (BL)	412	Ardownie & Ethiebeaton, andesite, 6,7,13,43, 51
Lake Superior, USA (BC, RC)	1100	Lincoln & Minneapolis, basalt, 2,3,8,13,14
Maddina, W. Australia (DN,GA)	2717	Fortescue Group, Maddina, basalt, 1,2,3,4,6

*Collectors are listed in the acknowledgements.
†Age references are given in Moxon and Carpenter (2009) and the cited literature.

polishing in large tumblers before export. Agates used in the study have not been tumbled or otherwise treated and are of two major types. The first is characterized by its white banding on an intense black background. A second type shows shades of pink and white; both types have been used in this study. Nova Scotia agates used in the study are black with extremely weak bands and could be confused with black flint. However a section examination reveals colourless banding flowing into a black background. The age of the Agate Creek host has not been determined but flora above and below the basalt host has been identified as Permo-Carboniferous and the agates are given a 'middle age' of 275 Ma. Agates are collected in a limited area of basalt following an old riverbed. The many colours make these generally small agates exceptionally attractive.

The discovery of agate in the neighbouring quarries of Ardownie and Ethiebeaton in eastern Scotland during the late 20th century was the first new agate area to be identified in Scotland for 100 years. The 412 Ma hosts contain attractive agates showing an intense blue with white banding achieving several cm in diameter. Lake Superior agates (1100 Ma) are found in gravel beds throughout the northern states in the USA and this wide distribution makes the agates one of the most commonly collected in the USA. Colour is limited with shades of orange-red to dark brown with an intense white banding being the most common; the agates can be large with sizes of 15 cm.

Archaean agates are from the Maddina basalt. Maddina agate 1 was found in a shallow meteorite impact crater and its physical properties were investigated for possible impact properties (Moxon *et al.*, 2006). Maddina samples 2 to 6 are from a restricted area. Apart from Maddina 1, Brazilian and Lake Superior agates, all the regional samples can be described as collections from a limited area.

Dehydration and rehydration experiments

The agate wall contact layer was removed and small slab samples were cut from individual slices. Initial runs were carried out on agates that had been left to acclimatize for 14 days in an air-conditioned preparation room. Part-way through the study, it was found that the water content in agate showed variations dependent upon the temperature and relative humidity (RH). On the basis of the standard deviation spread from the uncontrolled conditions, an approximate laboratory mid-RH value of 46% was selected for the start of a fresh investigation. This was achieved using a glycerol and water solution (Forney and Brandl, 1992). Samples were placed on wire gauze above the glycerol/ water solution and sealed in a plastic container that was positioned in two further plastic containers; each separated with static cold water jackets to minimize temperature variation. The final box was sealed and the temperature and relative humidity around the slabs were recorded in the agate-containing box every 4 h using a Sensormetrix Carbon LCD 61 data logger (accuracy ±0.5°C, ±2%RH). Additionally, five Brazilian agate slabs were kept as permanent controls with regular weighing

https://doi.org/10.1180/minmag.2017.081.002 Published online by Cambridge University Press

tracking any mass variations. Selective batches of five fresh slabs from each sample were further investigated after acclimatization at 100%RH; a separate set of Brazilian slabs was left in deionized water. Samples were checked weekly for seven weeks but again, constant mass was achieved after 14 days.

A 14 day programme for each stage was found to be sufficient for equilibration: (1) 46%RH acclimatization; (2) desiccator dehydration at laboratory temperatures; (3) rehydration at 46%RH; and (4) a final desiccator dehydration. Stage 3 was used to identify the mass of water that would re-enter the agate slabs; and stage 4 identified whether more water could be removed after a second dehydration. The full routine used five small slabs per agate and five agates per region; individual agate slabs weighed between 1–4 g. Powders were prepared from a single slab by repeated hand crushing and passing through a 50 μm sieve until ~3 g of powder was obtained. The powders also underwent acclimatization and desiccator dehydration. A Mettler M5 balance with an accuracy of ± 0.002 mg was used for all weighing.

High-temperature dehydration

High-temperature water loss using agates from the regions was found by heating small cuboids (~6 mm^3) and powders (< 50 μm). Mini-cuboids and powders were prepared from the same freshly cut section. An agate length of ~2 mm × 2 mm sectional area was cut using a diamond trim saw and sections cut to give ~2 g of mini-cuboids. After a 14 day acclimatization at 46%RH, ~0.6 g of each sample was heated in triplicate in capped platinum crucibles. The starting temperature was 600°C with a ramp rate of 20°C/min reaching a final temperature of 1200°C that was held for 90 min; test samples were run for a further 60 min. High-temperature water mass loss from triplicate sets of < 50 μm powders was determined after acclimatization and heating using the same conditions as the mini-cuboids. Comparative checks of the effect of particle size on the water loss at 1200°C were made with mini-cuboids (~6 mm^3), sieved grains (250–500 μm) and powders < 50 μm from six agates. Similar high-temperature investigations examined the dependence of water loss on cuboid volume. Cuboids with a volume of ~6 mm^3 and ~40 mm^3 were cut from seven agates. Individual cuboids were each prepared from a single slab and left to acclimatize for five days under uncontrolled conditions. The comparative heating tests were carried out in triplicate.

Scanning electron microscopy (SEM)

A JEOL 820 SEM has been used previously to examine freshly fractured, gold sputtered agates at 20 kV. Around 1000 micrographs of 60 agates found in basic igneous hosts with ages between 38 to 3477 Ma were available from the author's SEM library. Magnifications range from 50 to 20,000× and representative images have been selected to show the changes in morphology that occur as a result of ageing.

Calcite identification

Occasionally, powder XRD identifies traces of hidden calcite that has coexisted with α-quartz in agate. However, the Mexican Las Choyas agates have probably formed under unusual circumstances that are described later. Using XRD, ~50% of a previously examined batch was found to contain calcite. Tests were carried out using hydrochloric acid (~3 M) on two of the XRD identified calcite-containing agates from this region. Around 1 g of agate grains (250–500 μm) were prepared by crushing and sieving. The grains were placed in a 5 cm × 1.5 cm specimen tube and, when viewed from the side, the addition of 5 cm^3 of acid produced a slight but observable effervescence. The present study has examined 60 agate samples for their water content and 16 had been previously examined by XRD. The remaining 44 samples were tested for calcite using grains. It is essential that the grains are well washed with water as trace powder becomes a suspension and masks the effervescence.

Water terminology applied to agate

'Molecular water': is the water lost when finely powdered agate is heated >120°C; it is due to free and loosely bound water molecules. Available molecular water can be quantified by heating < 50 μm powders at a temperature between 130 and 190°C.

'Total water': is quantified by heating < 50 μm agate powders at temperatures ≥1000°C.

'Defect water': is the difference between the total water and molecular water. It is due to

https://doi.org/10.1180/minmag.2017.081.002 Published online by Cambridge University Press

tightly bound molecular water; isolated silanol groups linked to water; silanol groups linked by hydrogen bonding; and silanol groups in structural defects. The groups were identified by Yamagishi *et al.* (1997) and are discussed later.

'Desiccator dehydrated water': the water lost when agate slabs or powders have achieved a constant mass loss after 14 days desiccator dehydration.

'Mobile water': water that can enter and leave the agate but is dependent upon the surrounding water vapour pressure. Mobile water can be quantified after a second acclimatization following the initial desiccator dehydration.

'Trapped water': the mass difference between desiccator dehydrated water loss and mobile water. Trapped water is removed after desiccator dehydration but, under the uncontrolled ambient and the experimental 46%RH conditions, it is not returned on rehydration.

Results

Dehydration and rehydration experiments

Twelve cuboid slabs and four non-cuboid samples from the same Brazilian agate were prepared under uncontrolled conditions and left in a desiccator for 42 days with a re-weigh every 7 days. Dehydration losses were directly proportional to the slab mass and independent of the slab shape. A comparison of the percentage mass loss variation after 42 days and 14 days showed only third decimal place differences: 0.575(24)% and 0.570(23)%, respectively. Similar checks showed that the 14-day cycle of dehydration and rehydration routines were also within analytical error: limited to third decimal place differences.

All quoted mean data from the data logger are the mean values from each of the individual 4 h readings. Uncontrolled temperature and RH conditions in a small air-conditioned preparation room were recorded over 20 consecutive days and gave respective mean values of temperature and RH as 15.0(1.4)°C and 47(4)% producing a mean water vapour pressure of 810(94) Pa (data sheet, Wexler, 1976). The exercise was repeated for another 10 days when temperature and RH gave mean values of 18.7(2.7)°C and 41.5(5)%: a mean water vapour pressure of 875(125) Pa. Sample runs would be over a few months and the varied uncontrolled conditions demonstrated the need for temperature and RH control.

Acclimatization for the controlled experimental runs of the slab/powder samples required 18 weeks. During this period the acclimatized conditions recorded respective mean temperature and RH of 20.1(1.1)°C, 46(2)% with a mean water vapour pressure 1140(67) Pa: halving the standard deviation percentage of the uncontrolled conditions. Over the 18-week run, the five Brazilian agate control slabs produced a mean mass variation of 2.1923(2) g.

Desiccator dehydration water losses of the mean values from: (1) the young age group (excluding Brazil and New Zealand); (2) Brazil and New Zealand; and (3) middle/old-age hosts are 12(1)%, 21(1)% and 11(5)%, respectively, of the total available water (Table 2). The water returning to the agates after desiccator dehydration was determined after the second 46%RH acclimatization and was always less: mean values typically ~50% of the initial water lost. The agates from the Maddina basalt, Western Australia have probably experienced low-grade host-rock metamorphism and are discussed later as a special case.

Fresh slices from a selection of agates were examined at 20.1°C but at 100%RH. Samples from four Brazilian agates were also left in deionized water. It was expected that saturation acclimatization would take several weeks. However, constant mass was obtained after 14 days and assumed for all other slabs. Interestingly, the water content in the Brazilian agates was the same whether under water or held in the 100%RH atmosphere. Nine agates were compared at 46 and 100%RH. Only four showed an obvious greater water loss after 100% RH acclimatization (Table 4). However after dehydration, all agates from the nine samples held at 100%RH allowed the full return of the lost water; this is in contrast to the agates held under 46%RH or uncontrolled conditions (Tables 2 and 3).

Water mass differences between crushed powders and slabs were the prime objective in this study. Comparison of agate slabs and powders show, perhaps unsurprisingly, that the crushing process can result in some water losses. After 46% RH acclimatization, losses due to powder preparation are found using the mass difference between the desiccator slabs and powders. Brazil 64 and Mt. Warning 6, with a 0.25% difference, show the most extreme example of water mass loss due to powder under-reporting (Table 2).

https://doi.org/10.1180/minmag.2017.081.002 Published online by Cambridge University Press

TABLE 2. Dehydration and rehydration of slabs/powders. Dehydration of powders at 1200°C.

Sample	Desiccator (%) slabs/*powder*			1200°C (–) *powder* (%)	
	(–)1st Dehydration Slab/Powder	(+) Rehydration Slab	(–)2nd Dehydration Slab	Dehydration *Powder*	Total *Adjusted powder*
1) Australia, Mt. Warning, Queensland (23 Ma)					
1	0.15(1)/*0.07(1)*	0.14(1)	0.13(2)	*1.50(2)*	*1.58*
2	0.21(2)/*0.10(3)*	0.18(1)	0.16(0)	*1.62(1)*	*1.73*
6	0.37(3)/*0.12(4)*	0.20(1)	0.20(2)	*1.71(4)*	*1.96*
7	0.23(3)/*0.12(2)*	0.15(2)	0.14(2)	*1.60(1)*	*1.71*
8	0.15(2)/*0.07(0)*	0.09(1)	0.10(1)	*1.59(1)*	*1.67*
Mean	0.22(9)/*0.10(3)*	0.15(4)	0.15(4)	*1.60(8)*	*1.73(14)*
2) Mexico, Ojo Laguna (38 Ma)					
1	0.17(2)/*0.05(1)*	0.08(1)	0.11(2)	*1.76(2)*	*1.88*
12	0.20(2)/*0.08(1)*	0.09(1)	0.09(1)	*1.72(1)*	*1.84*
13	0.05(1)/*0.09(1)*	0.03(1)	0.03(1)	*1.07(4)*	*1.07*
15	0.16(1)/*0.03(2)*	0.12(1)	0.12(1)	*1.24(2)*	*1.37*
17	0.22(2)/*0.14(0)*	0.13(2)	0.13(2)	*1.39(3)*	*1.47*
Mean	0.16(7)/*0.08(4)*	0.09(4)	0.10(4)	*1.44(30)*	*1.53(34)*
3) Mexico, Las Choyas (45 Ma)					
6	0.16(2)/*0.08(1)*	0.11(1)	0.10(2)	*	*
9	0.29(1)/*0.06(0)*	0.09(1)	0.08(1)	*1.64(5)*	*1.87*
11	0.14(2)/*0.04(0)*	0.08(1)	0.07(1)	*0.98(3)*	*1.08*
15	0.22(5)/*0.08(1)*	0.11(2)	0.11(1)	*1.66(6)*	*1.80*
17	0.14(3)/*0.05(2)*	0.08(2)	0.08(2)	*1.02(1)*	*1.11*
Mean	0.19(6)/*0.06(2)*	0.09(2)	0.09(2)	*1.33(38)*	*1.47(43)*
4) Isle of Rum, Scotland (60 Ma)					
1	0.14(3)/*0.10(1)*	0.04(2)	0.07(2)	*1.16(0)*	*1.20*
2	0.24(1)/*0.03(1)*	0.05(1)	0.06(3)	*0.48(2)***	**
3	0.12(1)/*0.05(1)*	0.03(1)	0.05(1)	*1.15(3)*	*1.22*
12	0.16(2)/*0.21(4)*	0.05(1)	0.09(2)	*1.56(0)*	*1.56*
13	0.11(5)/*0.15(2)*	0.06(0)	0.07(2)	*1.34(3)*	*1.34*
Mean	0.15(5)/*0.11(7)*	0.05(1)	0.07(1)	*1.30(19)*	*1.33(17)*
5) New Zealand, Woolshed Creek (89 Ma)					
12	0.39(4)/*0.27(0)*	0.21(3)	0.18(3)	*1.39(1)*	*1.51*
13	0.33(1)/*0.20(0)*	0.14(0)	0.14(0)	*1.35(8)*	*1.48*
14	0.36(3)/*0.17(1)*	0.17(2)	0.16(1)	*1.58(4)*	*1.77*
17	0.29(3)/*0.27(4)*	0.14(2)	0.13(3)	*1.33(1)*	*1.35*
18	0.33(3)/*0.35(4)*	0.16(1)	0.17(1)	*1.49(3)*	*1.49*
Mean	0.34(4)/*0.25(7)*	0.16(3)	0.16(2)	*1.43(10)*	*1.52(15)*
6) Brazil, Rio Grande do Sul (133 Ma)					
12	0.34(1)/*0.15(2)*	0.15(0)	0.14(1)	*1.52(2)*	*1.71*
39	0.34(1)/*0.19(1)*	0.15(0)	0.15(1)	*1.39(3)*	*1.54*
64	0.43(2)/*0.18(4)*	0.16(1	0.13(1)	*1.42(2)*	*1.67*
72	0.29(2)/*0.21(1)*	0.20(2)	0.18(2)	*1.75(5)*	*1.83*
75	0.31(1)/*0.29(2)*	0.14(1)	0.14(1)	*1.56(1)*	*1.58*
Mean	0.34(5)/*0.20(5)*	0.16(2)	0.15(2)	*1.53(14)*	*1.67(11)*
7) Botswana, Semolale (180 Ma)					
33	0.03(1)/*0.02(0)*	0.02(1)	0.02(1)	*0.65(1)*	*0.66*
80	0.05(1)/*0.01(0)*	0.02(0)	0.02(1)	*0.59(2)*	*0.63*
112 (inner)	0.06(1)/*0.08(2)*	0.05(1)	0.04(0)	*0.68(2)*	*0.68*
114	0.05(1)/*0.05(1)*	0.02(1)	0.04(1)	*0.69(4)*	*0.69*
152	0.03(0)/*0.02(1)*	0.02(0)	0.02(0)	*0.81(2)*	*0.82*

(continued)

https://doi.org/10.1180/minmag.2017.081.002 Published online by Cambridge University Press

TABLE 2. (*contd*.)

Sample	Desiccator (%) slabs/*powder*			1200°C (–) *powder* (%)	
	(–)1st Dehydration Slab/Powder	(+) Rehydration Slab	(–)2nd Dehydration Slab	Dehydration *Powder*	Total *Adjusted powder*
Mean	0.04(1)/*0.04(3)*	0.03(1)	0.03(1)	*0.68(8)*	*0.70(7)*
112 (outer)	0.13(0) nt	0.08(1)	0.07(1)	nt	
8) Canada, Bay of Fundy, Nova Scotia (202 Ma)					
11	0.11(3)/*0.03(1)*	0.06(0)	0.08(1)	*0.72(0)*	*0.80*
21	0.08(1)/*0.04(2)*	0.05(1)	0.04(2)	*0.55(3)*	*0.59*
24	0.09(1)/*0.06(3)*	0.07(1)	0.07(2)	*0.75(1)*	*0.78*
25	0.17(2)/*0.06(2)*	0.09(1)	0.13(1)	*0.73(1)*	*0.84*
30	0.13(1)/*0.13(0)*	0.09(1)	0.08(3)	*1.12(1)*	*1.12*
Mean	0.12(4)/*0.06(4)*	0.07(2)	0.08(3)	*0.77(21)*	*0.83(19)*
9) Australia, Agate Creek (275 Ma)					
104	0.06(1)/*0.00(0)*	0.05(1)	0.04(1)	*0.54(1)*	*0.60*
108	0.11(2)/*0.00(0)*	0.02(0)	0.04(0)	*0.52(0)*	*0.63*
122	0.09(1)/*0.03(0)*	0.06(0)	0.06(0)	*0.54(1)*	*0.60*
140	0.10(1)/*0.06(5)*	0.06(1)	0.06(1)	*0.71(1)*	*0.75*
142	0.09(1)/*0.04(0)*	0.05(0)	0.05(1)	*0.59(2)*	*0.64*
Mean	0.09(2)/*0.03(3)*	0.05(2)	0.05(1)	*0.58(8)*	*0.64(6)*
10) Scotland, East Midland Valley (412 Ma)					
Ard' 6	0.07(2)/*0.07(2)*	0.02(1)	0.02(1)	*0.54(3)*	*0.54*
Ard' 7	0.08(1)/*0.07(1)*	0.01(1)	0.02(1)	*1.13(2)***	**
Eth'13	0.15(2)/*0.03(2)*	0.06(1)	0.05(1)	*0.50(2)*	*0.62*
Eth 43	0.06(1)/*0.06(0)*	0.02(1)	0.02(1)	*0.48(2)*	*0.48*
Eth 51	0.07(1)/*0.08(2)*	0.02(1)	0.03(1)	*0.65(2)*	*0.65*
Mean	0.09(4)/*0.06(2)*	0.03(2)	0.03(1)	*0.54(8)*	*0.57(8)*
11) USA, Lake Superior (1100 Ma)					
2	0.06(2)/*0.03(1)*	0.03(1)	0.03(2)	*0.59(1)*	*0.62*
3	0.02(0)/*0.04(0)*	0.02(0)	0.01(1)	*0.45(3)*	*0.45*
8	0.07(2)/*0.05(0)*	0.03(2)	0.02(2)	*0.93(2)*	*0.95*
13	0.06(2)/*0.08(2)*	0.03(1)	0.02(1)	*0.71(1)*	*0.71*
14	0.03(1)/*0.04(0)*	0.01(0)	0.01(0)	*0.90(10)*	*0.90*
Mean	0.05(2)/*0.05(2)*	0.02(1)	0.02(1)	*0.72(20)*	*0.73(21)*
12) Australia, Maddina (2717 Ma)					
1	0.00(0)/*0.04(1)*	0.01(0)	0.01(1)	*0.20(2)*	*0.20*
2	0.00(0)/*0.02(2)*	0.02(0)	0.00(0)	*0.14(2)*	*0.14*
3	0.03(2)/*0.01(2)*	0.01(0)	0.01(0)	*0.37(1)*	*0.39*
4	0.00(0)/*0.01(1)*	0.00(0)	0.00(0)	*0.14(3)*	*0.14*
6	0.00(0)/*0.00(0)*	0.00(0)	0.00(0)	*0.24(1)*	*0.24*
Mean	0.01(1)/*0.02(2)*	0.01(1)	0.00(1)	*0.22(9)*	*0.22(10)*

Slab data (standard), *powder data* (italics). Total adjusted powder data is found by adding any water lost during powder crushing (see text). *High temperature data invalid due to trace calcite; **outlier data that is excluded from the respective means; nt – data not taken. The regional numbers are also used in Figs 1 and 4; individual sample numbers are the collection numbers.

High temperature dehydration

Unexpected results were produced by the high-temperature mass losses from mini-cuboids compared to powders. Water loss due to powder preparation was at its greatest in the younger agates and the use of mini-cuboids was intended to compensate for powder losses. A total of 30 different agate mini-cuboids were compared at

https://doi.org/10.1180/minmag.2017.081.002 Published online by Cambridge University Press

TABLE 3. Water losses from agate slabs and mini-cuboids.

Sample*	Desiccator			1200°C**
	(–)1st dehydration	(+)rehydration	(–) 2nd dehydration	(–)dehydration
Brazil 64(a)	0.57(2)	0.25(2)	0.25(2)	1.45(1)
Brazil 64(b)	0.43(2)	0.16(1)	0.13(1)	1.25(5)
Brazil 75(a)	0.53(6)	0.25(2)	0.22(2)	1.45(4)
Brazil 75(b)	0.31(1)	0.14(2)	0.14(2)	1.38(2)
Brazil 12(a)	0.46(2)	0.24(1)	0.24(1)	1.50(2)
Brazil 12(b)	0.34(1)	0.15(0)	0.14(1)	1.34(0)
NZ W Sh12(a)	0.34(5)	0.13(1)	0.12(1)	1.51(2)
NZ W Sh12(b)	0.39(4)	0.21(3)	0.18(3)	1.20(2)
NZ W Sh18(a)	0.45(2)	0.20(3)	0.22(3)	1.42(2)
NZ W Sh18(b)	0.33(3)	0.16(1)	0.17(1)	1.30(3)
Mex LCh 6(a)	0.15(2)	0.11(1)	0.11(1)	0.86(6)
Mex LCh 6(b)	0.16(2)	0.11(1)	0.10(2)	0.86(1)
Mex LCh 9(a)	0.22(4)	0.09(1)	0.09(1)	0.83(5)
Mex LCh 9(b)	0.29(1)	0.09(1)	0.08(1)	0.71(3)
Bots' 33(a)	0.05(1)	0.03(0)	0.03(0)	0.61(5)
Bots' 33(b)	0.03(1)	0.02(1)	0.02(1)	0.68(2)
Bots' 112(a)	0.06(1)	0.02(1)	0.04(1)	0.61(5)
Bots' 112(b)	0.06(1)	0.05(1)	0.04(0)	0.41(3)
Ag'Cr'104(a)	0.06(1)	0.04(1)	0.04(1)	0.53(3)
Ag'Cr'104(b)	0.06(1)	0.05(1)	0.04(1)	0.46(5)
Ard'7 (a)	0.08(1)	0.01(1)	0.03(0)	0.99(4)
Ard'7 (b)	0.08(1)	0.01(1)	0.02(1)	0.99(6)

*(a) Samples kept under uncontrolled conditions; (b) samples equilibrated at a RH of 46% and temperature 21°C.
**Data from 1200°C dehydration are from mini-cuboids.

1200°C with < 50 μm powders. Overall, 21 of 30 test samples showed greater high-temperature dehydration from powders with just three mini cuboid samples showing a greater loss. Insufficient heating was not the reason for this cuboid under-reporting; extended 150 min heating in test samples did not produce further mass loss. Data from the 30 cuboids and powder samples are given in Table 1s. (Tables 1s to 3s are supplemental, have been deposited with the Principal Editor of *Mineralogical Magazine* and are available from http://www.minersoc.org/pages/e_journals/dep_mat_mm.html).

A comparative check of the effect of particle size on water loss at 1200°C was made with a collection of six agates from three regions using powders < 50 μm, grains 250–500 μm and mini-cuboids (~6 mm^3). Mass losses from the mini-cuboids and 250–500 μm grains were similar in three of the six agates but would have under-reported the < 50 μm powders by up to 29% (Table 2s deposited). However, there was little variation in the water-loss mean relative standard deviation for the respective cuboids, grains and powder: 1.8(6)%, 1.8(12)%, 2.0(7)%. Additional tests were carried out on seven agates using two ranges of cuboid sizes: ~6 mm^3 and ~40 mm^3. The percentage mass loss was shown to be independent of the volume in six agates. Indications from these limited samples suggest that larger cuboids would produce a marginally greater water-loss mean relative standard deviation: 3.2(25)% compared to 2.5(14)% from the smaller cuboids (Table 3s deposited).

Where powder preparation water losses are identified, compensatory additions are made to the 1200°C powder losses and the new value is then treated as the total water content (Table 2). Thus, the 1200°C powder loss from Brazil 64 was 1.42% and the powder preparation water-loss difference found between slab and powder is 0.25%: a total water content of 1.67%. The study has involved 60 agate samples from the 12 regions and major mean data outliers at 1200°C are limited to two samples: Isle of Rum (#2) and Ardownie, Scotland (#7). They produce a total water data compared to their regional means that are, respectively, ~35% and

https://doi.org/10.1180/minmag.2017.081.002 Published online by Cambridge University Press

~100% greater. The high-temperature data for these two agates have not featured in the quoted means in Table 2 and subsequent plots. The remaining plots have used all the available data.

Calcite identification

Unfortunately, XRD showed that one of the Las Choyas agates contained hidden calcite traces. However, the use of hydrochloric acid on the crushed grains of the 44 samples that had not been examined by XRD did not produce any effervescence.

Discussion

Water content in agate after acclimatization at 46%RH

The majority of investigators of agate/chalcedony water content have either not been aware, or have not acknowledged that the water content in agate varies with the atmospheric water vapour pressure. Sample descriptions are limited to the powder particle size or the state of the slab and its thickness. Nevertheless, comment on agate water variation with temperature and RH is not new. Flörke *et al.* (1982) examined the water content of Brazilian agates using two sets of temperature and water vapour pressure described as 'cave climate' and 'room climate' conditions. Unfortunately, the equilibration time and the method of recording the water vapour pressure were not given.

Under the present study conditions, desiccator dehydration is a measure of the water loss from interconnected structural defects and can only be a fraction of the available molecular water. Mobile water is due to water that can enter and leave the agate and varies with the number of suitable pathways and the surrounding atmospheric water vapour pressure. The nature of the trapped water has not been examined here, but is probably loosely hydrogen-bonded water clusters or water with weak silanol links; collectively they are in equilibrium with mobile water molecules. A possible order of water loss during desiccator dehydration would be the departure of free molecular water, followed by individual water molecules from clusters held around connected inter-granular regions and defect sites that have links to exit routes. Evidence for this two-component water loss is demonstrated by the rehydration and the second dehydration (Table 2). Only part of the lost water re-enters the agate on rehydration and this same mass is then totally removed on the second dehydration (data columns 2 and 3, Table 2). Thus, Mt. Warning #2 shows a desiccator dehydration loss of 0.21% with mobile water content of 0.18%: trapped water content of 0.03%.

Trapped water changes over the geological time scale as demonstrated by 0.17% in the Mt. Warning #6 agate (23 Ma) to as little as 0.01% in the Botswana #112 agate (180 Ma) (Table 2). However as a fraction of the desiccator dehydrated water, the proportion of trapped water is similar in young and middle/old age agates: 48(17)% and 47(21)% respectively. Nevertheless, subsequent exposure at 100%RH for 14 days shows it is possible for the returning rehydration water molecules to swamp the pathways and return all the lost water (Table 4).

Agate water content after acclimatization at 100%RH and uncontrolled conditions

Over time, basic agate hosts become more porous and subject the gas vesicles and any agates to solutions of silica and trace ions. Exposure to 100%RH was intended to identify the maximum mass of water that could be contained by the agates. The outcome provided unexpected results: the same percentage water content is found whether the samples are left under water or exposed to a 100%RH atmosphere. Furthermore, only four of the nine agates tested produced an obvious greater water content at 100%RH compared to those at 46%RH (Table 4). The failure to show an increase in the agate water content after 100%RH exposure in some of the samples has two possible causes. After preparation and cutting, the samples went from uncontrolled conditions with a proportion of water clusters leaving limited space for the entry of fresh water molecules. Also at 100%RH, the samples are exposed to water that will have multiple hydrogen-bonded water links in both the liquid and vapour states. Such water clusters will have reduced access to the agate microstructure; this particularly applies to the middle/old age agates because of a reduction in access routes. These water restrictions at 100%RH are demonstrated by two Brazilian agates (#64 and 75) having a greater water content after 2 weeks under uncontrolled conditions than 7 weeks exposure at 100%RH (Tables 3 and 4). On the basis of this limited evidence, the mobile water content in agate increases with increasing RH until some value before 100%RH is reached. After this point, water clustering restricts further access.

By default, data obtained under an uncontrolled laboratory environment and 46%RH controlled

https://doi.org/10.1180/minmag.2017.081.002 Published online by Cambridge University Press

TABLE 4. Water content in agate samples acclimatized at 46% $_{(46)}$ and 100%RH$_{(100)}$. Brazilian samples left in deionized water $_{(aq)}$.

Sample	Desiccator		
	(–)1st dehydration	(+)rehydration	(–) 2nd dehydration
Br 75$_{(100)}$	0.44(2)	0.45(2)	0.42(4)
Br 75$_{(aq)}$	0.42(3)	0.42(4)	nt
Br 75$_{(46)}$	0.31(1)	0.14(1)	0.14(1)
Br 72$_{100)}$	0.29(4)	0.25(3)	0.25(4)
Br 72$_{(aq)}$	0.33(2)	0.33(4)	nt
Br 72$_{(46)}$	0.29(2)	0.20(2)	0.18(2)
Br 39$_{(100)}$	0.48(3)	0.46(3)	0.48(3)
Br 39$_{(aq)}$	0.48(1)	0.45(2)	nt
Br 39$_{(46)}$	0.34(1)	0.15(0)	0.15(1)
Br 64$_{(100)}$	0.50(3)	0.48(3)	0.47(3)
Br 64$_{(aq)}$	0.48(3)	0.45(1)	nt
Br 64$_{(46)}$	0.43(2)	0.16(1)	0.13(1)
WSh 17$_{(100)}$	0.32(5)	0.29(3)	nt
WSh 17$_{(46)}$	0.29(3)	0.14(0)	0.13(3)
L Ch 15$_{(100)}$	0.28(1)	0.31(3)	0.31(1)
L Ch 15$_{(46)}$	0.22(5)	0.11(2)	0.11(1)
Bots 80$_{(100)}$	0.11(1)	0.10(1)	0.10(1)
Bots 80$_{(46)}$	0.05(1)	0.02(0)	0.02(1)
Ag Cr 140$_{(100}$	0.08(1)	0.08(3)	0.10(1)
Ag Cr 140$_{(46)}$	0.10(1)	0.05(1)	0.05(1)
Ethie 51$_{(100)}$	0.11(3)	0.11(3)	0.13(3)
Ethie 51$_{(46)}$	0.07(1)	0.02(1)	0.03(1)

nt – data not taken.

conditions can be compared. These differences are most acute with agates from host regions with ages <180 Ma, e.g. desiccator dehydration for Brazil 75 showed an increase in the dehydrated water from the controlled conditions 0.31(1)% to 0.53(6)% in uncontrolled conditions. Due to partial pathway closures, there are minimal dehydrated water differences between the middle age and old age agates (Table 3).

Effect of the agate sample size on the water content

Infrared has been used to investigate the water dehydration process at 500°C in chalcedony slabs with a thickness of 138 to 234 μm (Fukuda *et al.*, 2009). They showed that water mass changes are mainly due to the loss of molecular water with the bulk of the silanol water untouched. Silanol resistance to an even higher temperature dehydration is shown in the present study where, regardless of the white porous appearance of the mini-cuboids after heating, the <50 μm powders generally produce a greater water loss. Cuboid under reporting was found in 21 of the 30 test samples with only three mini-cuboids showing a larger loss. Although powder preparation can result in some water loss, the crushing process clearly opens more water pathways allowing a greater silanol water loss.

Limited tests have been carried out on seven agates using two cuboid volumes: ~6 mm^3 and ~40 mm^3. Although the percentage mass loss in each agate pair were within range for six samples, the larger cuboids produced a marginally greater mean relative standard deviation water loss at ~3.2(25)% compared to ~2.5(14)% in the smaller cuboids. These differences suggest that individual samples within the larger cuboids possibly offer a varied silanol protection at high-temperature dehydration (Table 3s deposited).

Quantification of water in agate and chalcedony using TGA

A thermogravimetric profile of powdered agate tracks mass losses with respect to temperature. The

https://doi.org/10.1180/minmag.2017.081.002 Published online by Cambridge University Press

plot shape to ~120°C shows an initial loss due to molecular and some loosely hydrogen-bonded water but over the next ~80°C there is minimal mass change. Above 350°C, further dehydration occurs when more tightly bound molecular water is lost (Yamagishi *et al.*, 1997).

Final dehydration of the silanol groups is complete ~1000°C (e.g. Yamagishi *et al.*, 1997). These distinct dehydration divisions allow prolonged box-oven powder heating at temperatures between ~130 to 190°C allowing quantification of molecular and weakly hydrogen-bonded water in hydrated silica minerals (e.g. Herdianita *et al.*, 2000*a*; Moxon and Ríos, 2004). The latter study used 4 h oven heating at 170°C to determine free water in <50 μm agate powders. Furnace heating of fresh <50 μm powders at 1200°C gave the total water and the mass loss difference between the two temperatures was treated as defect water. Plots of water loss as a function of host-rock age showed the molecular water was independent of age. The mean defect water from the 14 agate regions studied, indicated a general decrease with respect to host-rock ages <400 Ma.

The present study raises questions on the validity of water data in the Moxon and Ríos (2004) study and agate/ chalcedony water quantification from elsewhere? Unfortunately, very few of the 2004 agates are of a suitable size for the multiple demands of the present work. This study is limited to 12 regions but fair comment can be made about the water loss trends from the 2004 study. Water loss differences due to powder preparation are greatest with agates from young hosts and without correction there will be an inevitable under-reporting. In the 2004 study, the free water in agate was shown to be independent of host-rock ages e.g. both Iran (50 Ma) and Lake Superior (1100 Ma) agates produced similar low free-water content. However, the 2004 study did not take into account any water loss due to powder preparation that is now noteworthy in younger agates. The younger agates do show water trends that are discussed later but any water corrections from hosts >180 Ma would be negligible. The original study stated that defect water showed a general decrease with agates from hosts aged <400 Ma; this is now shown to occur later at <180 Ma (Table 2).

Water content in agate and host-rock age

Age-related trends in physical properties and SEM observations suggest that agates have a common start, following the same initial growth mechanism. Agates then evolve with a similar development over geological time. Hence on formation, agates from the same area should trap similar masses of water at around the same geological time and subsequent changes should be roughly comparable. All the agates, except those from Brazil, Lake Superior and Maddina 1, were collected from restricted areas and provide a valid test for this hypothesis.

Desiccator dehydration provides a measure of mobile and trapped water and with standard deviation included; the data spread comparisons show that all the individual mean values of the 60 desiccator-dehydrated slabs were lying inside their respective regional mean. Comparisons of individual mobile water data show that rehydration followed by the second dehydration are the same and can only be due to the entry and then the loss of an equivalent mass of atmospheric water (Table 2). Again with standard deviation included, each of the individual mean water entry and exit values is within range of the regional mean: demonstrating that agates from the same region provide similar collective pathway access for water movement. Pathway changes in all agates over host ages 23 to 1100 Ma progress similarly.

The changes in mobile water show there has been considerable structural closure between 60 and 180 Ma (Table 2). Quartz crystallite size and mobile water also show an age-related sequence of changes (Figs 1*a* and *b*): (A) Initially, a linear decrease in mobile water content is matched by a linear increase in quartz crystallite growth over the first 60 Ma; (B) a cessation in quartz growth and mobile water content for the next ~200 Ma; (C) an increase in quartz crystallite growth over the next ~40 Ma and finally; (D) minimal change in both mobile water content and quartz development over the next~800 Ma. Mobile water is limited to open pathways and cannot be the cause of the quartz crystallite coarsening that occurs throughout the agate; this is discussed later.

Atypical properties of Brazilian and New Zealand agates

Agates from Brazil and New Zealand are exceptions in the crystallite age-related trends (Fig. 1*a*). Their high mobile water also shows off-trend behaviour. The young age agate category shows an increasing host age from Australia (23 Ma) through to New Zealand (89 Ma) and Brazil (135 Ma). Previously determined mogánite content and quartz crystallite size data has been obtained from agates in 26 regions. Only agates from Brazil, New Zealand and

https://doi.org/10.1180/minmag.2017.081.002 Published online by Cambridge University Press

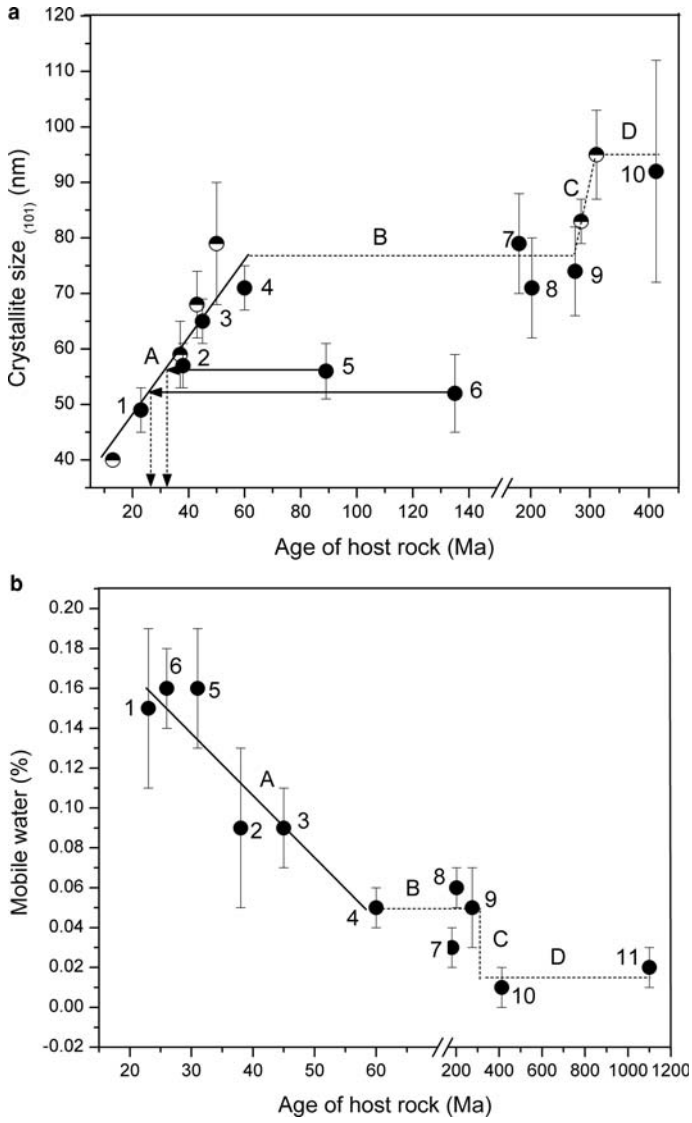

FIG. 1. (*a*) Crystallite size as a function of host-rock age. The plot shows 16 regions with host ages <450 Ma; agate regions used in the present study are shown by numbered solid circles. Agates from Brazil and New Zealand are plot outliers suggesting respective agate formation ages of 26 and 31 Ma. Data after Moxon and Carpenter (2009). (*b*) Mobile water is a measure of the open water pathways and shown as a function of host-rock age. The plot shows agates from 11 of the 12 regions used in the present study; agate data from New Zealand [5] and Brazil [6] at their crystallite size ages from Fig. 1*a*. Note the four-step sequence (A to D) of changes in both plots. Dashed lines are for eye guidance. The agate hosts used in the present study (solid circles) and host ages are: [1] Mt. Warning, Queensland, Australia (23 Ma); [2] Ojo Laguna, Mexico (38 Ma); [3] Las Choyas, Mexico (45 Ma); [4] Rum, Scotland (60 Ma); [5] Woolshed Creek, New Zealand (89 Ma); [6] Rio Grande do Sul, Brazil (135 Ma); [7] Semolale, Botswana (180 Ma); [8] Bay of Fundy, Nova Scotia, Canada (202 Ma); [9] Agate Creek, Australia (275 Ma); [10] East Midland Valley, Scotland (412 Ma); [11] Lake Superior (1100 Ma).

https://doi.org/10.1180/minmag.2017.081.002 Published online by Cambridge University Press

one English region were outliers with higher mogánite content and lower crystallite size than suggested by their host-rock age (Moxon and Carpenter, 2009). For the respective Brazilian and New Zealand agates, quartz crystallite size would suggest a formation age of ~26 and ~31 Ma (Fig. 1*a*). The present off-trend total water differences for the same two regions provide further evidence of a later agate formation. Here, mobile water indicates a younger age than the 38 Ma Mexican Laguna agate host. Later plots (including Fig. 1*b*) have replaced host-rock age for the Brazilian and New Zealand agates by the proposed respective 26 and 31 Ma crystallite size ages shown in Fig. 1*a*).

Causes of calcite in Las Choyas agates and vertical cracks in Maddina agates

Sectioned agate can reveal obvious visible mineral inclusions with macrocrystalline quartz, clay minerals and calcite being the most frequent. Mogánite and α-quartz are usually the only minerals identified in the agate section using powder XRD. On occasions, hidden calcite is identified in agate from basic igneous hosts. When found, calcite is usually a 'one-off' as other agates from the same area are generally calcite free. In a previous study, 180 agates from 26 regional hosts were examined using XRD (Moxon and Carpenter, 2009). Only seven agates contained trace calcite and four were from the Las Choyas region. The difficulty of trace calcite and silica coexisting within agate is shown by the lack of calcite, even when the circumstances are most favourable. Two of the best-known agate limestone hosts in the USA are the St Louis Limestone Formation, Missouri (Union Rd agates) and the Minnelusa Limestone Formation, S. Dakota (Fairburn agates). Powder XRD examination of 8 Union Road agates and 18 Fairburn agates have been obtained previously and only two contained calcite (Moxon, unpublished data). This high frequency of trace calcite in the Las Choyas agates indicates an atypical formation.

The Las Choyas agates are the only group that does not occur in a basic igneous host but is found in the vitric tuff of the 45 Ma Liebres Formation. Agates from this region have been examined previously for mogánite content and crystallite size. Both determinations showed that the Las Choyas agates were within the trend for agates from basic igneous hosts that were slightly younger and older (Fig. 1*a*). The current work shows the desiccator dehydrated water content from the Las Choyas (45 Ma) agates and the Laguna (38 Ma) are also on-trend (Table 2). Nevertheless, the frequent occurrence of calcite in these agates does suggest an unusual event during formation that is probably not linked to the nature of the host. Keller *et al.* (1982) produced a stratigraphic section of the Sierra del Gallego area that includes the Las Choyas and Laguna agate. They describe the Liebres Formation as a poorly-bedded conglomerate of limestone cobbles, volcanic fragments and unconsolidated silt. Around 9 Ma after the Liebres host formation, there was an intrusion by the Mesteño rhyolite. It is probable that solutions from this incursion are the silica source for the trace calcite found in these uniquely-shaped spherical geodes. However, agates are not found in the Mesteño rhyolite itself (Cross pers. comm.).

The new Maddina agates gave an opportunity to compare the water content of Maddina samples (2 to 6) with Maddina 1. The latter agate has been investigated in detail as part of a study of agates from Western Australian hosts >1.8 Ga (Moxon *et al.*, 2006). Maddina 1 was found in a shallow impact meteorite crater and was examined for possible unique impact properties. Infrared scans on Maddina 1 doubly polished slabs between 50–200 μm in thickness demonstrated near-zero agate water with limited structural silanol water. The data from the present batch of Maddina agates would concur with those findings: producing near-zero desiccator dehydrated water, and minimal high-temperature water losses (Table 2).

Agates found in the Maddina Basalt Fortescue Group are generally dark brown due to iron oxy-hydroxides. An examination of thick and thin sections of these Maddina agates reveals vertical cracks in all samples (e.g. Figs. 2*a,b*). The crystal structure of agate does not have any areas of weakness that can explain the vertical fracturing; random fractures in agates can generally be assigned to host-rock movement. The Fortescue Group shows low-grade metamorphism that is probably due to burial ~2.45–2.0 Ga (Nelson *et al.*, 1992). For these Maddina agates, the unusual fracturing can be best explained by external metamorphic pressure applied from the top or bottom or both directions. Hence, a date for the origin of Maddina agates is between 2.0 Ga and the host age of ~2.72 Ga.

Genesis and age-related development of agate found in basic igneous hosts

The silica source

The origins of the silica source, method of transportation and the physical state of the initial

https://doi.org/10.1180/minmag.2017.081.002 Published online by Cambridge University Press

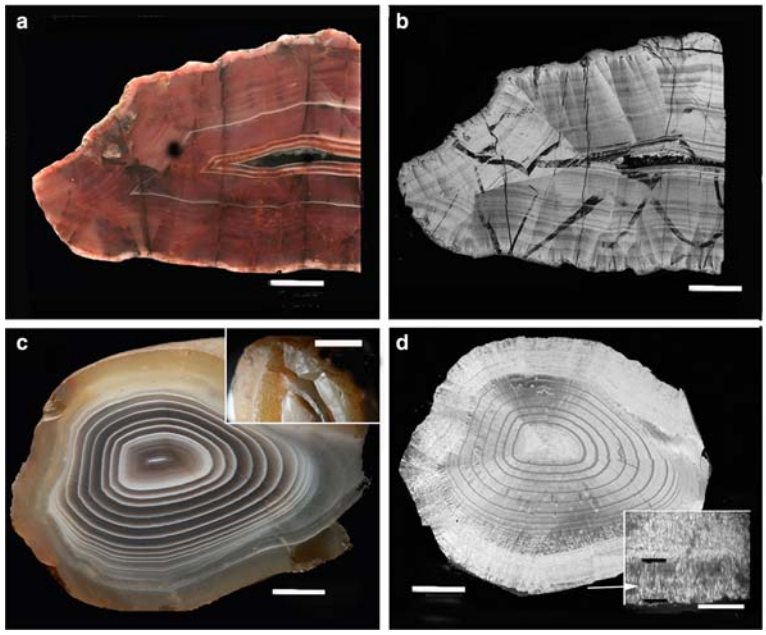

FIG. 2. (*a*) Maddina 3 showing the contrasting lighter coloured wall contact layer and vertical cracks. (*b*) The same slab of Maddina 3 in thin section demonstrating the sweeping chalcedonic fibrosity that mostly runs from the outer edge to the centre of the agate. (*c*) Botswana 112 is an unusual agate by showing a clean fracture between the brown region and the black and white centre. The fracture is shown on the extreme right and insert. (*d*) A thin section of the same agate showing a less pronounced fibrosity than in Maddina 3. The insert shows the contrasting microtexture of the wall contact band against the lighter texture of the bulk of the agate. Figs 2*b* and *d* with polars crossed; scale bars for the whole agates = 1 cm; Fig 2*c* insert = 5 mm; Fig. 2*d* insert = 1 mm.

silica deposits are all unknown. Agate has never been made in the laboratory and there have been few attempts to extrapolate laboratory data back to normal earth surface conditions. Over the past 200 years, all possible means of silica entry into the gas vesicle have been considered: osmosis; hot springs; alternating wet and dry seasons; late hydrothermal activity; host-rock weathering; re-melting of chert xenoliths; silica immiscibility within the magma; silica gel formation leading to the well-known Liesegang phenomena. Unfortunately, every proposal presently creates unanswerable objections; these problems have been reviewed and discussed in great detail (Landmesser (1984), Moxon (1996), Götze (2011).

There has only been one attempt to deal with the time lag between host and agate/chalcedony formation in basic igneous hosts. Water percolation through the host-rocks in the Yucca Mountain, Nevada, USA produced initial chalcedony deposits ~4 Ma after the formation of the 13 Ma volcanic tuff (Neymark *et al.*, 2002). Another study using agate data from 26 regions showed, apart from the three previously named regions, approximate trends of quartz crystallite size and mogánite content with links to the host-rock age (Moxon and Carpenter, 2009). This combined data supports a hypothesis that agate formation is generally around the same geological time as the host formation (Fig. 1*a*). Of the 26 agate regions studied, only agates from Cumbria, England and Western Australia had suffered post host-formation metamorphism (Moxon and Carpenter, 2009 and references therein). Hence, metamorphic activity is not considered a primary silica source for agate formation. However, at least two of the agate host-rocks in the present study show intense mineral weathering and the subsequent host-rock porosity would allow silica solutions to permeate the gas vesicles. The giant Paraná basalt flow is the primary host of Brazilian agate but sufficient host-rock has decomposed to create a major secondary agate source in surrounding fields (Matsui *et al.*, 1974). The same authors identified the water in Brazilian

https://doi.org/10.1180/minmag.2017.081.002 Published online by Cambridge University Press

agates as meteoric. Thin sections of the Devonian Scottish agate hosts show a high degree of weathering with the mafic minerals remaining only as faint structural ghosts (Moxon, 1996).

The Yucca Mt. observations and the identification of host weathering sustain an agate genesis hypothesis based upon silica deposition from solution: a view supported by most of the scientific literature published over the last 25 years (e.g. Heaney, 1993; Landmesser, 1998; Götze, 2011; Hartmann *et al.*, 2012; Moxon *et al.*, 2013). There is less of a consensus whether the first silica deposit is an amorphous powder or a gel. Gel cannot diffuse through the solid host rock and an alternative gel creation model was suggested by Harder (1993). He proposed that a gel formed within the vesicle cavity after a reaction between silica solutions and aqueous trivalent cations. An electron microprobe analysis of nine Brazilian combined horizontal and wall-lining agates found that Fe^{3+} was always below detection limits and Al^{3+} was below 100 ppm in four of the samples (Moxon *et al.*, 2013). It is unlikely that these low concentrations could combine with an equally low silica concentration to produce a gel. Unless silica gels are surrounded by water, they dehydrate within weeks and leave an amorphous powder. There seems little reason to speculate on this gel formation route.

Is the agate wall contact layer the first or last silica deposit?

The agate and gas vesicle wall contact layer has long been recognized as different from the rest of the agate and is regarded as the 'first generation'. In a sectioned agate, this 1–2 mm wall-contact layer typically shows as a different colour. Occasionally, the layer may appear to be absent although a thin section will reveal its presence as a different microtexture. Maddina 3 agate is typical and shows colour as well as micro-textural differences (Fig. 2*a*). The relationship between the wall contact band and the agate bulk raises an imponderable genesis question: how does fresh silica pass through a wall of chalcedony?

Chalcedony-lined amethyst geodes have led to suggestions that later silica solutions diffuse through the first chalcedony layer (Proust and Fontaine, 2007) or, solution transport occurs through chalcedony fractures (Commin-Fischer *et al.*, 2010). These are two recent propositions by those who assume the contact band is the 'first generation'. A thin section examination of the wall contact layer in the wall-lining type of agate shows that the layer is uniform in microtexture and thickness. There is never any evidence of gravity producing a thicker layer at the base of the agate (e.g. Fig. 2*a*). Indeed it would be remarkable if an initial silica deposit, in whatever form, could evenly coat the gas vesicle wall. An alternative hypothesis is based on the development of agates following the diagenetic changes listed in sequence 1. If amorphous silica undergoes diagenesis through the listed polymorphs then, an initial fixed mass of the less dense silica precursors would undergo bulk shrinkage. Fresh silica could be added throughout each stage and continue to maintain a full vesicle. The problem was discussed in a recent study of simple Brazilian agates having horizontal bands in the lower section and wall-lining bands in the upper chamber (Moxon *et al.*, 2013).

Thin sections of four different agates showed the discrete horizontal bands either had a thinner or no wall contact band, whereas a thicker contact band was present in the upper chamber containing the single unit of wall-lining agate. It was argued that if diagenesis followed sequence 1 then the shrinkage changes would affect the more voluminous upper chamber to a greater extent. Diagenesis would permit fresh silica inputs and eventually form a wider band in the upper chamber. These changes were observed in the agates studied allowing the proposition that the wall-contact band is really the 'last generation'.

Further evidence for the 'last generation' wall contact is suggested by the present study. An examination of Botswana 112 shows an apparent ~5 mm wall contact band (Fig. 2*c*). However, sufficient of the true wall contact band has survived the thin-section grinding and shows the wall contact microtexture difference is still only ~1 mm (insert in Fig. 2*d*). A fracture in Botswana 112 shows a clean natural break between the outer brown and the inner layers. This atypical poor section adhesion and colour change demonstrates that in this agate, the inner and brown regions formed as separate entities (Fig. 2*c* and insert).

A thin section of Botswana 112 reveals three contrasting microtextures: the actual ~1 mm wall contact band, the rest of the brown band and a final inner area (Fig. 2*d* and insert). The presently described trends in age-related water show higher water content is indicative of younger material. The slab water content data in the brown band shows the desiccator dehydration and following rehydration respectively at ~2 and ~1.5 times greater than the

https://doi.org/10.1180/minmag.2017.081.002 Published online by Cambridge University Press

inner area (Table 2). Hence, the brown band is the penultimate deposit with a proposed shrinkage allowing a final silica input creating the ~1 mm of the 'last generation' wall contact band.

Similarities and differences between chert, silica sinter and agate

A good body of literature is available on chert and silica sinter genesis studies; their development reveals similarities with agate and chalcedony. Chalcedony can form in sinter but sinter sedimentologists tend to bring all forms of microcrystalline quartz under the quartz heading and comparisons with agate are less obvious. Some links between the silica sinter diagenesis (sequence 1) and agate formation have already been given. However, any attempts to make the agate link produce some major differences. The time scale for sinter digenesis completion is typically ~50 ka (Herdianita *et al.*, 2000*b*) but more significant is the possibility of an even faster conversion of sinter into quartz. In these high-temperature waters, a partial conversion into quartz has occurred within weeks (Lynne *et al.*, 2006). Such times are too short for agate formation.

Contrarily, the chert time scale is too long for a direct application to agate. Chert diagenesis is prolonged and an initial amorphous silica deposit can survive in surface rocks for up to 85 Ma. Further conversion along the genesis pathway to cristobalite/tridymite occurs after 5–10 Ma but it is still observed in rocks up to 120 Ma, whereas quartz formation requires a minimum of 30–40 Ma (Hesse, 1988). As agate has been identified in hosts as young as 23 Ma (Mt. Warning, Australia), and chalcedony is found in the 13 Ma Yucca Mt., a chert diagenesis-time scale cannot have a direct application to agate. Comparative temperature-time scale considerations would place agate between sinter and chert and this is in line with the relative formation temperatures of these three silica minerals. Scottish and Namibian agate formation temperatures have been identified for these respective regions at ~50°C (Fallick *et al.*, 1985) and 39–85°C (Saunders, 1990).

Although mogánite is commonly found in silica sinter, chert and agate, the mogánite survival rates differ greatly. Mogánite transforms into quartz but again, the diagenesis process is linked to different time scales. In sinters with ages 20 to 200 ka, the mogánite content is at a maximum of <13%, whereas Tertiary sinters are generally mogánite free (Rodgers and Cressey, 2001). Chert hosts of Cretaceous age have been identified with a mogánite survival >20% (Heaney, 1995). Flints, also Cretaceous age, from Norfolk, England have a 14–18% mogánite content (Zhang and Moxon, 2014). By contrast, chalcedony from the 13 Ma Yucca Mt. contains 56% mogánite and mogánite has been identified in agate from an 1100 Ma host (Moxon and Carpenter, 2009).

Silica sinter discharges from weakly alkaline chloride-rich waters at temperatures ≤100°C; the mogánite preservation differences would, once again, appear to be linked to temperature and/or the growth mechanism and/or the different microstructure. In the present study, some silanol water has survived in agate mini-cuboids after heating at 1200°C for up to150 min. The retention of trace mogánite in agate for at least 1100 Ma must be due to the ability of the agate microstructure to fix and retain some of the silanol water and mogánite. Mogánite can be found in the ~300 Ma Union Road limestone-hosted agates from the St Louis limestone, USA (Moxon, unpublished data). Although agate in limestone hosts is limited in the world agate order, the formation of agate rather than chert in limestone is a problem that has never been examined.

Agate: a mineral that develops with age

Changes in agate age-related surface morphology have been shown using the SEM (Moxon, 2002). Surface differences between agates from Brazil (host age 135 Ma, but here, agates are given a proposed age ~26 Ma), and Scotland (412 Ma host age) are shown in Fig. 3. The agate ageing process is demonstrated by a sharpening in the white band structure and the increasing size of the globules in the non-white bands. The freshly fractured surface of the Brazilian agate (Fig. 3*a*) appears as a mixture of broken layered regular sections creating flattened hollows with globules ~0.1 μm in diameter. The globules are more apparent after a ten fold increase in magnification to 20,000× with their presence around the added white circle (Fig. 3*b*). Globular development continues and after ~400 Ma, globules are ~1 μm in diameter (Fig. 3*c*). The white bands in agate also show trends starting with a weak layered structure in the Brazilian agate (Fig. 3*d*) but display development in the Mull agate (60 Ma host, Fig. 3*f*`). White band growth continues and is well developed in the 412 Ma Scottish agate (Fig. 3*e*).

The reaction between silanol water and mogánite is the essential key for the development of quartz

https://doi.org/10.1180/minmag.2017.081.002 Published online by Cambridge University Press

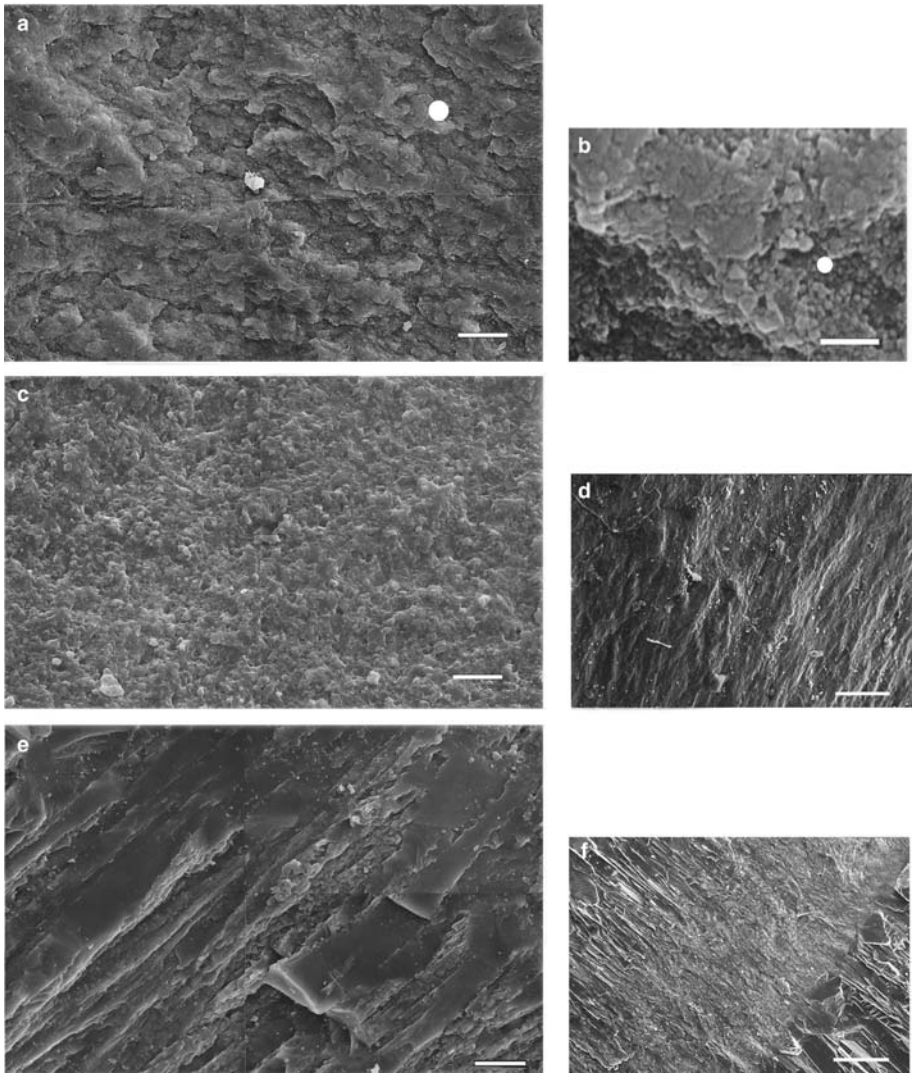

FIG. 3. SEM micrographs showing: (*a*) Pale brown band in a Brazilian agate. (*b*) Small globules can be seen in the 10-fold magnification around the added white circle that is also shown in 3*a*. (*c*) After a further ~390 Ma, well-developed globular growth is shown in the light blue band of this agate (Ardownie, Scotland). (*d*) White bands in Brazilian agate generally show poor development. (*e*) The white banding is fully developed in the Ardownie, Scotland agate (412 Ma). (*f*) After ~60 Ma, a distinct structural change has occurred in the white bands of this Isle of Mull agate (upper left and bottom right). Figs 3*a, c, e*, are montage assemblies each from four individual micrographs; scale bars 3*a*, *c*, *e* = 10 μm; 3*b* = 1 μm; 3*d*, *f* = 100 μm.

crystallites in agate. The release of water is demonstrated by cathodoluminescence where an age-related decrease in the relative intensity of the red emission band (~660 nm) is matched by an increase in the relative intensity of the orange emission band (~620 nm). The similar magnitude of plots of the changing relative intensities as a function of $\log_{10}$ (host-rock age) demonstrates this relationship: –0.17 (red) and 0.15 (orange). Changes in the respective red and orange emission bands are indicators of the loss of silanol bonds producing an increase in the strained Si–O–Si bonds. (Moxon and Reed, 2006 and references therein). Later work suggests the strained Si–O–Si

https://doi.org/10.1180/minmag.2017.081.002 Published online by Cambridge University Press

bond has formed via Si–O· ·Si (Stevens-Kalceff, 2013).

$$Si–O–H + H–O–Si \rightarrow Si–O–Si + H_2O \quad (2)$$

An investigation of the laboratory transformation of mogánite to quartz using small agate rods in sealed gold tubes added support for the observed agate development under normal Earth surface conditions, albeit via a different mechanism (Moxon and Carpenter, 2009). Water was not added and quartz development relied on the release and retention of free and silanol water after heating up to 550°C at 100 MPa pressure. Plots of decreasing mogánite content and increasing quartz crystallite size with respect to time, produced approximate mirror images. The key role of water for this crystallite growth was further demonstrated when similar agate rods were heated in an open furnace at 550°C for 122 days but only showed limited development. In the study, a cessation of quartz growth is observed in the agate rods that were heated between 350–500°C; producing links with growth cessation when agates age under normal Earth surface conditions (Fig. 1*a*).

Heated agates become cracked and porous leading to an increase in water pathways and in the high-temperature study, the quartz growth cessation was attributed to Zener pinning. A phenomenon that prevents further growth when a second phase (mogánite) existing within a polycrystalline matrix (α-quartz) is able to exert a restraining force on the quartz crystallite boundary.

Over the geological time scale, released water from the silanol groups dissolves the more soluble mogánite leading to silica recrystallization as α-quartz. Water pathways are prime sites for the new quartz; now supported by evidence of their partial closure in agates from the middle/old age hosts (Table 2). Development cannot be limited solely to the water pathways and quartz growth must occur throughout the agate. Further evidence for quartz development over the first ~60 Ma and links between water and mogánite are shown in Figs 1*a* and 4*c*. Growth cessation occurs when the mogánite content is ~4% (Fig. 4*c*). The plot of mogánite as a function of total water content (Fig. 4*c*) shows a linear change over the first 60 Ma with respective mean data decreases of mogánite and total water from 19% and 1.73% (#1 Mt. Warning, Australia) to 9% and 1.47% (#3 Las Choyas, Mexico) with data from Rum (#4) shown as an outlier.

The total water content of agates from hosts with ages between 180 and 1100 Ma is variable between 0.83 and 0.57% but this is not matched by a corresponding change in mogánite content that remains ≈4(1)% (Fig. 4*c*). The agate pathways in these middle/old age hosts have been reduced by ~70% but the most probable cause of growth cessation is a wide distribution of the remaining 4% mogánite together with a reduction of suitable nearby silanol groups. Age groups show trapped water differences but trends within the groups have not been found (Fig. 4*a*). However, total water as a function of host-rock age and crystallite size as a function of total water show clear trends in agates from hosts <60 Ma (Figs 4*b* and 4*d*).

Apart from time scales and mogánite content differences, there are sufficient trends and similarities between sinter, chert and agate. During the diagenetic process, silica sinter and chert show a general decrease in the water and mogánite content with an increasing density and crystallinity. Developing agate is comparable, albeit over a different time scale. Although the initial conditions for agate formation are unknown, potential silica polymorph precursors have occasionally been identified: cristobalite/tridymite layering in Brazilian agates (Flörke *et al.*, 1982) and cristobalite in agates from Mexico and Iran (Moxon and Carpenter, 2009). It is significant that these findings are limited to agates from younger hosts. Ageing completes the diagenetic process and accounts for the failure to detect any silica precursors in agates from older hosts. The findings of the present study add to the agate genesis model based on sequence 1 that was first proposed by Landmesser (1995, 1998).

Will the enigma of agate genesis be solved in the next 200 years?

It is unlikely that agates will be made in the laboratory but a deeper insight into the question of agate genesis might result from a study of agates from hosts with ages <10 Ma. Extrapolation of data obtained under the present controlled conditions would suggest that agates of this age should have the following water contents: total water of ~1.81(6)%; mobile water of 0.20(2)%. Similarly, extrapolation of data in Fig. 1*a* back to zero time produces a quartz crystallite size of ~33(8) nm. Caution is needed as extrapolation of mogánite content (excluding Yucca Mt., Nevada) and desiccator-dehydrated water back to zero time

https://doi.org/10.1180/minmag.2017.081.002 Published online by Cambridge University Press

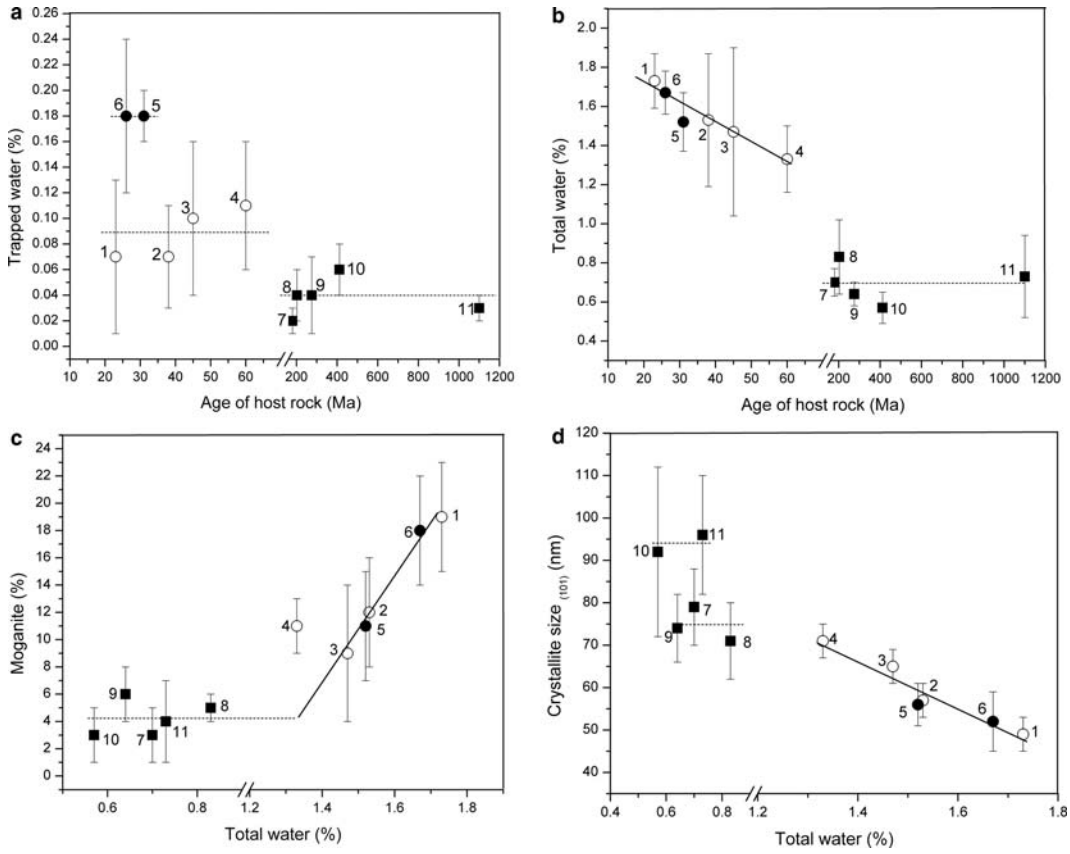

FIG. 4. (*a*) Plot of trapped water as a function of host age divides the agate regions into three groups: Brazil and New Zealand and agate regions < and > 60 Ma. (*b*) Total water as function of host-rock age. Differentiation between middle and old age agate hosts cannot be made. (*c*) Mogánite content as a function of total water. A linear decrease in mogánite content from young agates leads to an approximately constant mogánite content at ~4% in agates from hosts older than ~180 Ma. Agate region 4 (Rum) has been treated as an outlier. (*d*) Quartz crystallite size as a function of total water conveniently divides the agates into young and middle age with the greater crystallite size separating the old age agates. Dashed lines are for eye guidance. Middle/old age agates (solid squares); young agates excluding those from Brazil and New Zealand (open circles); Brazil and New Zealand (solid circles). All Fig. 4 plots use the crystallite age of the Brazilian and New Zealand agates as determined from Fig. 1*a*. Individual agate host regions have the same numbers as given in Fig. 1. Mogánite content and quartz crystallite size data after Moxon and Carpenter (2009).

(excluding Brazil and New Zealand agates) produces values of 21(4)% and 0.25(4)% respectively. However, these have already been exceeded with the 56% mogánite content in chalcedony from the Yucca Mt. (13 Ma) and the 0.34% of desiccator dehydrated water from Brazilian and New Zealand agates. Development in the early years could be more rapid with linear changes occurring much later than the initial agate formation. All water data is dependent on the water vapour pressure and propositions here are using the controlled conditions of the present study.

Industrial requirements and links with early life forms have produced a long history of funding and scientific investigation into silica sinter and chert. Over the last 40 years, agate studies have lacked any equivalent incentives. However, this might change as Mars Rover units are now providing infrared data on hydrated silica minerals found on the Martian surface. Earth-bound investigations are covering the whole range of silica-rich minerals, including chalcedony, in an attempt to aid remote data identification of the Martian silica (e.g. Rice *et al.*, 2013). Other investigators have looked at

https://doi.org/10.1180/minmag.2017.081.002 Published online by Cambridge University Press

the possibility that chalcedonic filamentous fabrics might exist on Mars, perhaps providing links with water and microbiological activity (Hofmann and Farmer, 2000). However as demonstrated here, water interpretation will require care as at least one of the hydrated silica minerals can produce a widely variable water content that is dependent upon age of formation, particle size and the surrounding water vapour pressure.

Conclusion

Brazil is the world's largest agate exporter and samples are easily available in size and number providing a ready access for scientific studies of agate properties. However, the water content in Brazilian agates is particularly vulnerable to changes in RH leading to water content fluctuations. The study has demonstrated differences in respective desiccator dehydrated and total water up to 71% and 14% from Brazilian agates kept under uncontrolled conditions and the chosen 46%RH controlled conditions. Such wide variations show that for water quantification data to have validity, agate and chalcedony should be first acclimatized under known settings.

The Brazilian and New Zealand agates show that the agate host-rock age is not always an approximation for the age of the agate. A simple 14-day desiccator dehydration of weighed slabs and crushed powders from the same agate slab will show whether powder preparation will have any effect on the water content losses.

Comparable water pathways form in agates from the same region: these conduits then become systematically healed by the development of fresh quartz over the geological time scale. The study has shown that mobile and total water has, for different reasons, links with the quartz development. The Brazilian (135 Ma) and New Zealand (89 Ma) agates yield high identical mean desiccator dehydration and mobile water data adding further to the proposition that agates from these two regions formed much later than the host-rock age. The magnitude of the determined water data and previously obtained mogánite content and quartz crystallite size provides evidence that the agates from Brazil and New Zealand formed earlier than the 38 Ma of the Mexican Laguna agates.

Powders (<50 μm) heated at 1200°C generally produce a greater water loss than mini-cuboids and 250–500 μm grains demonstrating that the latter two sizes continue to retain a proportion of the silanol water. This silanol water retention in slabs has implications for high-temperature water quantification using infrared where doubly polished slabs, up to 1 mm thick, have been used. Brazilian agate mini-cuboids and 250–500 μm grains underreported water mass losses obtained from <50 μm powders by up to 22%. Much depends upon research intentions but if valid water quantification is the concern, slab silanol water retention and water losses due to powder preparation is a problem that needs attention.

Water has a dual role in the origin and later development of agate. It is most probable that silica enters the gas vesicles in an aqueous solution. Secondly, agate development continues with the help of released silanol water dissolving mogánite that later recrystallizes as α-quartz. The variously defined water contents show age-related trends in agates up to ~60 Ma. The present study has produced water data that concurs with previous work showing ~60 Ma as the starting age for growth cessation that now includes water content as well as quartz crystallite development. After acclimatization, the desiccator offers the possibility of approximately placing agate-dating limits. Under the present set of experimental conditions, desiccator dehydrated water loss > or < 0.14% would suggest agate hosts < or > 60 Ma respectively.

Acknowledgements

The study has only been possible because of the generous donation of agate by research workers, collectors, and agate processing firms from around the world. I am much obliged to David Anderson, Glenn Archer (Outback Mining, Australia), Jeannette Carrillo (Gem Center USA, Inc.), Roger Clark, Nick Crawford, Brad Cross, Robin Field, Gerhard Holzhey, Brian Isfield, Herbert Knuettel (Agate Botswana), Reg Lacon, Brian Leith, Maziar Nazari, Dave Nelson, Leonid Neymark, John Raeburn, John Richmond, Vanessa Tappenden, Bill Wilson and Johann Zenz. I am indebted to the Dept. of Earth Sciences, Cambridge University for access to the High Temperature and Pressure Laboratory and to Chris Parish for effective furnace management. Maarten Broekmans, Jens Götze and Assistant Editor Martin Lee are thanked for their constructive reviews of the manuscript.

References

Commin-Fischer, A., Berger, G., Polvé, M., Dubois, M., Sardini, P., Beaufort, D. and Formoso, M. (2010)

https://doi.org/10.1180/minmag.2017.081.002 Published online by Cambridge University Press

Petrography and chemistry of SiO_2 filling phases in the amethyst geodes from Sierra Geral Formation deposit, Rio Grande do Sul, Brazil. *Journal of South American Earth Sciences*, **29**, 751–760.

Fallick, A.E., Jocelyn, J., Donelly, T., Guy, M. and Behan, C. (1985) Origin of agates in the volcanic rocks of Scotland. *Nature*, **313**, 672–674.

Flörke, O.W., Köhler-Herbertz, B., Langer, K. and Tönges, I. (1982) Water in microcrystalline quartz of Volcanic Origin: Agates. *Contributions to Mineralogy and Petrology*, **80**, 324–333.

Forney, C.F. and Brandl, D.G. (1992) Control of humidity in small controlled – environment chambers using glycerol-water solutions. *HortTechnology*, **2**, 52–54.

Fukuda, J., Yokoyama, T. and Kirino, Y. (2009) Characterization of the states and diffusivity of intergranular water in a chalcedonic quartz by high temperature in situ infrared spectroscopy. *Mineralogical Magazine*, **73**, 825–835.

Götze, J. (2011) Agate-fascination between legend and science. Pp. 20–133 in: *Agates III* (J. Zenz, editor). Bode, Lauenstein, Germany.

Götze, J., Nasdala, L., Kleeberg, R. and Wenzel, M. (1998) Occurrence and distribution of 'moganite' in agate/chalcedony: a combined micro-Raman, Rietveld, and cathodoluminescence study. *Contributions to Mineralogy and Petrology*, **133**, 96–105.

Götze, J., Tichomirowa, M., Fuchs, H., Pilot, J. and Sharp, Z.D. (2001) Geochemistry of agates: a trace element and stable isotope study. *Chemical Geology*, **175**, 523–541.

Harder, H. (1993) Agates-formation as a multicomponent colloid chemical precipitation at low temperature. *Neues Jahrbuch für Mineralogie – Monatschefte*, **1993**, 31–38.

Hartmann, L.A., Duarte, L.C., Massone, H-J., Michelin, C., Rosenstengel, L.M., Theye, T., Pertile, J., Arena, K.R., Duarte, S.K., Pinto, V.M., Barboza, E.G., Rosa, M.L.C.C. and Wildner, W. (2012) Sequential opening and filling of cavities forming vesicles, amygdales, and giant amethyst geodes in lavas from the southern Paraná volcanic province, Brazil and Uruguay. *International Geology Review*, **54**, 1–14.

Heaney, P.J. (1993) A proposed mechanism for the growth of chalcedony. *Contributions to Mineralogy and Petrology*, **115**, 66–74.

Heaney, P.J. (1995) Moganite as an indicator for vanished evaporates: a testament reborn? *Journal of Sedimentary Research*, **A65**, 633–38.

Hemantha Kumar, G.N., Parthasarathy, G. Chakradhar, R.P.S., Lakshmana Rao, J. and Ratnakaram, Y.C. (2010) Temperature dependence on the electron paramagnetic resonance spectra of natural jasper from Taroko Gorge (Taiwan). *Physics and Chemistry of Minerals*, **37**, 201–208.

Herdianita, N.R., Rodgers, K.A. and Browne, P.R.L. (2000*a*) Routine instrumental procedures to characterise the mineralogy of modern and ancient silica sinters. *Geothermics*, **29**, 65–81.

Herdianita, N.R., Browne, P.R.L., Rodgers, K.A. and Campbell, K.A. (2000*b*) Mineralogical and textural changes accompanying ageing of silica sinter. *Mineralium Deposita*, **35**, 48–62.

Hofmann, B.A. and Farmer, J.D. (2000) Filamentous fabrics in low-temperature mineral assemblages: are they fossil biomarkers? Implications for the search for a subsurface fossil record on the early Earth and Mars. *Planetary and Space Science*, **48**, 1077–1086.

Hesse, R. (1988) Origin of chert: Diagenesis of biogenic siliceous sediments. *Geoscience Canada*, **15**, 171–192.

Keller, P.C., Bockoven, N.T. and McDowell, F.W. (1982) Tertiary volcanic history of the Sierra del Gallego area, Chihuahua, Mexico. *Geological Society of America Bulletin*, **93**, 303–314.

Knauth, L.P. (1994) Petrogenesis of chert. Pp. 233–258 in: *Silica* (P.J. Heaney, C.T. Prewitt and G.V. Gibbs, editors). Reviews in Mineraology, **29**. Mineralogical Society of America, Washington DC.

Landmesser, M. (1984) Das problem der Achatgenese. *Mitteilungen Pollichia*, **72**, 5–137, Bad Dürkheim/ Pflaz [English Abstract].

Landmesser, M. (1995) "Mobility by metastability": silica transport and accumulation at low temperatures. *Chemie der Erde*, **55**, 149–176.

Landmesser, M. (1998) "Mobility by metastability" in sedimentary and agate petrology: applications. *Chemie der Erde*, **58**, 1–22.

Lynne, B.Y., Campbell, K.A., Perry, R.S., Browne, P.R.L. and Moore, J.N. (2006) Acceleration of sinter diagenesis in an active fumarole, Taupo volcanic zone, New Zealand. *Geology*, **34**, 749–752.

Matsui, E., Salti, E. and Marini, O.J. (1974) D/H and $^{18}O/^{16}O$ ratios in waters obtained from the basaltic province of Rio Grande do Sul, Brazil. *Geological Society of America Bulletin*, **85**, 577–580.

Moxon, T. (1996) *Agate Microstructure and Possible Origin*. Terra Publications, Doncaster, UK, 106 pp.

Moxon, T. (2002) Agate: a study of ageing. *European Journal of Mineralogy*, **14**, 1109–1118.

Moxon, T. and Carpenter, M.A. (2009) Crystallite growth kinetics in nanocrystalline quartz (agate and chalcedony). *Mineralogical Magazine*, **73**, 551–568.

Moxon, T. and Reed, S.J.B. (2006) Agate and chalcedony from igneous and sedimentary hosts aged 13 to 3480 Ma: a cathodoluminescence study. *Mineralogical Magazine*, **70**, 485–498.

Moxon, T. and Ríos, S. (2004) Moganite and water content as a function of age in agate: an XRD and thermogravimetric study. *European Journal of Mineralogy*, **16**, 269–278.

https://doi.org/10.1180/minmag.2017.081.002 Published online by Cambridge University Press

Moxon, T., Nelson, D.R. and Zhang, M. (2006) Agate recrystallisation: evidence from samples found in Archaean and Proterozoic host rocks, Western Australia. *Australian Journal of Earth. Sciences*, **53**, 235–248.

Moxon, T., Reed, S.J.B. and Zhang, M. (2007) Metamorphic effects on agate found near the Shap granite, Cumbria, England: as demonstrated by petrography, X-ray diffraction and spectroscopic methods. *Mineralogical Magazine*, **71**, 461–476.

Moxon, T., Petrone, C.M. and Reed, S.J.B. (2013) Characterization and genesis of horizontal banding in Brazilian agate: an X-ray diffraction, thermogravimetric and electron microprobe study. *Mineralogical Magazine*, **77**, 227–248.

Nelson, D.R., Trendall, A.F., de Laeter, J.R., Grobler, N.J. and Fletcher, I.R. (1992) A comparative study of the geochemical and isotopic systematics of late Archaean flood basalts from the Pilbara and Kaapvaal Cratons. *Precambrian Research*, **54**, 231–256.

Neymark, L.A., Amelin, Y., Paces, J.B. and Peterman, Z. E. (2002) U-Pb ages of secondary silica at Yucca Mountain, Nevada: implications for the paleohydrology of the unsaturated zone. *Applied Geochemistry*, **17**, 709–734.

Proust, D. and Fontaine, C. (2007) Amethyst geodes in the basaltic flow from Triz quarry at Ametista do Sul (Rio Grande do Sul, Brazil): magmatic source of silica for the amethyst crystallizations. *Geology Magazine*, **144**, 731–739.

Rice, M.S., Cloutis, E.A., Bell III, J.F., Bish, D.L., Horgan, B.H., Mertzman, S.A., Craig, M.A., Renaut, R.W., Gautason, B. and Mountain, B. (2013) Reflectance spectra of silica- rich materials: Sensitivity to environment and implications for detections on Mars. *Icarus*, **223**, 499–533.

Rodgers, K.A. and Cressey, G. (2001) The occurrence, detection and significance of moganite (SiO_2) among some silica sinters. *Mineralogical Magazine*, **65**, 157–167.

Rodgers, K.A., Browne, P.R.L., Buddle, T.F., Cook, K.l., Greatrez, R.A., Hampton, W.A., Herdianita, N.R., Holland, G.R., Lynne, B.Y., Martin, R., Newton, Z., Pastars, D., Sannazarro, K.L. and Teece, C.I.A. (2004) Silica phases in sinters and residues from geothermal fields of New Zealand. *Earth Science Reviews*, **66**, 1–61.

Saunders, J.A. (1990) Oxygen-isotope zonation of agates from Karoo volcanic of the Skeleton Coast, Namibia: Discussion. *American Mineralogist*, **75**, 1205–1206.

Schmidt, P. (2014) What causes failure (overheating) during lithic heat treatment. *Archaeological and Anthropological Sciences*, **6**, 107–112.

Schmidt, P., Slodczyk, A., Léa, V., Davidson, A., Puaud, S. and Sciau, P. (2013) A comparative study of the thermal behaviour of length-fast chalcedony, length-slow chalcedony (quartzine) and moganite. *Physics and Chemistry of Minerals*, **40**, 331–340.

Stevens-Kalceff, M. (2013) Cathodoluminescence microanalysis of silica and amorphized quartz. *Mineralogy and Petrology*, **107**, 455–469.

Wexler, A. (1976) Vapor pressure Formulation for water in the range 0 to 100°C. A revision. *Journal of Research of the National Bureau of Standards-A Physics and Chemistry*, **80A**, 775–785.

Yamagishi, H., Nakashima, S. and Ito, Y. (1997) High temperature infrared spectra of hydrous microcrystalline quartz. *Physics and Chemistry of Minerals*, **24**, 66–74.

Zhang, M. and Moxon, T. (2014) Infrared absorption spectroscopy of SiO_2-moganite. *American Mineralogist*, **99**, 671–680.

https://doi.org/10.1180/minmag.2017.081.002 Published online by Cambridge University Press